Local Chain Motion of *Isotactic* and *Syndiotactic* Poly(methyl methacrylate)s Studied by the Fluorescence Depolarization Method

Keiko Ono, Tsuyoshi Sasaki, and Masahide Yamamoto*

Division of Polymer Chemistry, Graduate School of Engineering, Kyoto University, Sakyo, Kyoto 606, Japan

Yumi Yamasaki, Koichi Ute, and Koichi Hatada

Department of Chemistry, Faculty of Engineering Science, Osaka University, Toyonaka, Osaka 560, Japan

Received July 28, 1994; Revised Manuscript Received January 3, 1995[⊗]

ABSTRACT: The local chain motion of *syndiotactic* and *isotactic* poly(methyl methacrylate)s (*s*-PMMA and *i*-PMMA) was examined by the time-resolved fluorescence depolarization method. The reduced relaxation time, T_m/η, and its activation energy, E^*, were measured in various solvents. Both the T_m/η and E^* for *s*- and *i*-PMMAs decreased with a decrease in the local segment density. As for the effect of the stereoregularity, the activation energy of both PMMAs showed similar values, but the relaxation time of *s*-PMMA was ca. 1.5–2.0 times larger than that of *i*-PMMA. Such a difference in relaxation time is closely related to the static chain stiffness predicted by the helical wormlike (HW) chain model.

Introduction

Many kinds of motional modes in polymer chain dynamics[1-3] have been examined by various spectroscopic techniques, e.g., NMR,[4,5] ESR,[6,7] dielectric relaxation,[8,9] neutron scattering,[10] dynamic light scattering,[11] and fluorescence depolarization methods.[12-14] The polymer chain in a dilute solution undergoes a local conformational transition with a time scale from 10^{-9} to 10^{-10} s, and the scale of the motional mode is smaller than that represented by Rouse et al.[1]

We used the fluorescence depolarization technique to clarify the local motion in a polymer chain. In this method, a fluorescent probe is introduced at a specific position in a polymer chain, and the chain local motion is evaluated by the measurement of an anisotropy ratio. We have examined the local motion in various kinds of polymers, i.e., polystyrene and its derivatives (poly(α-methylstyrene) and poly(*p*-methylstyrene)),[15,16] poly(alkyl methacrylate)s (alkyl = methyl, ethyl, isopropyl; PMMA, PEMA, and P*i*PMA, respectively),[17,18] and *cis*-polyisoprene.[19] For polystyrenes,[16] the substituted methyl group increases both the mean relaxation time and the activation energy.

For poly(alkyl methacrylate)s, the relaxation time increases in the order of PEMA, PMMA, and P*i*PMA. Previously,[18] we indicated that the mean relaxation time depends on not only the bulkiness of the alkyl residue but also the stereoregularity of the polymer. However, the detailed relationship between the chain dynamics and the stereoregularity has not yet been clarified. Previously, Yamakawa et al.[20-22] proposed a helical wormlike (HW) chain model. The HW model is described by four parameters, κ_0, τ_0, M_L, and λ^{-1}, where κ_0 and τ_0 are the curvature and the torsion on taking the characteristic helix, M_L is a molecular weight per unit contour length, and λ^{-1} is a stiffness parameter of the HW chain. They estimated[21] λ^{-1}(*i*-PMMA) = 32.7 Å and λ^{-1}(*s*-PMMA) = 65.6 Å, and they demonstrated the existence of a large difference in the static chain stiffness between *i*-PMMA and *s*-PMMA. From the dynamic standpoint, Iwasa et al.[23] examined the dielectric behavior of an *i*-PMMA (*I*:*H*:*S* = 96:3:1) and a *s*-rich PMMA (*I*:*H*:*S* = 7:26:67) in toluene and dioxane solutions by the method of dielectric relaxation. They reported that the relaxation time of *s*-rich PMMA is ca. 4 times longer than that of *i*-PMMA. Hatada et al.[24] examined the relaxation time of poly(α-substituted acrylate)s in a solution by ^{13}C and ^{1}H NMRs. They also reported that the *isotactic* polymer chain is more flexible than the *syndiotactic* one. Herein, we studied the dynamic properties of *i*-PMMA and *s*-PMMA in dilute solutions by the fluorescence depolarization technique and discuss in detail the effect of stereoregularity on the local motion of a chain.

Table 1. Molecular Weight, Its Distribution, and Triad Tacticity (%) of Labeled Polymer Samples

	$M_n \times 10^{-4}$	M_w/M_n	*S*	*H*	*I*
s-PMMA	2.1	1.11	86	14	0
i-PMMA	2.5	1.24	0	0	100

Experimental Section

Preparation of the Anthracene-Labeled PMMA Samples. The sample of the anthracene-labeled *s*-PMMA was obtained by the procedure described in a previous paper.[17] The data of the molecular weight and tacticity of the sample are given in Table 1.

The anthracene-labeled *i*-PMMA was prepared in the following manner based on the living isotactic polymerization[25] of triphenylmethyl methacrylate (TrMA). Polymerization of TrMA (9.13 mmol) was initiated with 9-fluorenyllithium (0.122 mmol) in THF (30.4 mL) at −78 °C. After 4 h, 9,10-bis(bromomethyl)anthracene (0.073 mmol) dissolved in THF (21.7 mL) was added to the solution of the living poly(TrMA) anions. The mixture was stirred for 2 h at −78 °C, for an additional 36 h at −20 °C,[26] and then for 24 h at room temperature. Finally, the reaction was terminated with a small amount of methanol, and the mixture was poured into 1.0 L of methanol. The methanol-insoluble part (90.1% yield) was collected by centrifugation, washed several times with methanol, and dried in vacuo for 3 h at 40 °C. The poly(TrMA) was converted to PMMA by hydrolytic cleavage of the triphenylmethyl groups (refluxing for 1 h in 5% HCl/methanol) and subsequent methylation with diazomethane in dry benzene. Figure 1a

[⊗] Abstract published in *Advance ACS Abstracts,* June 1, 1995.

0024-9297/95/2228-5012$09.00/0

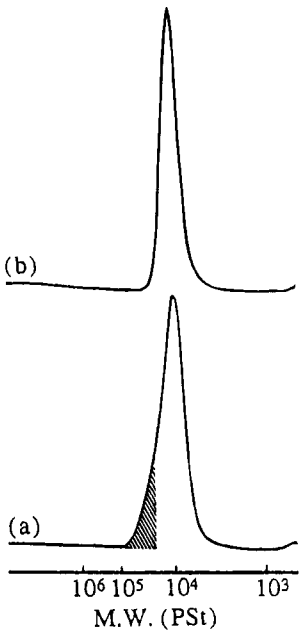

Figure 1. GPC curves of the anthracene-labeled *i*-PMMA (a) and the *i*-PMMA prepared by a control experiment (b). The shaded part of a was separated by repeated fractionation.

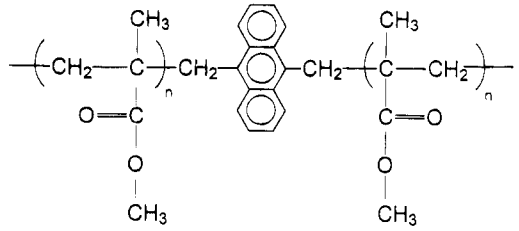

Figure 2. PMMA sample labeled with anthracene in the middle of the main chain.

shows the GPC curve of the resultant PMMA (M_n = 1.07 × 10^4, M_w/M_n = 1.34). The GPC curve has a discernible shoulder at the higher molecular weight side of the main peak. Such a shoulder was not observed in GPC analysis of the PMMA sample (M_n = 1.04 × 10^4, M_w/M_n = 1.14) prepared by a control experiment (Figure 1b). The control experiment was carried out in a way similar to that described above except that the polymerization of TrMA was terminated without the addition of 9,10-bis(bromomethyl)anthracene. The shoulder part in Figure 1a was separated by repeated fractionation with preparative GPC (column, Shodex k-2003, 20 i.d. × 300 mm; eluent, chloroform, 4.0 mL/min). The fraction was found to be almost perfectly isotactic by 500-MHz ^{1}H-NMR and to have a M_n 2.4 times as large as that of the control PMMA (Table 1). The absorption spectrum of the fraction in acetonitrile (0.03 wt %) showed the peaks due to the anthracene unit (An) at 350–425 nm and those due to the fluorenyl end groups (Fl) at 300–305 nm (Figure 2). From the intensity ratio of the peaks at 378 and 302 nm, the relative content of An to Fl in the *i*-PMMA sample was determined to be An:Fl = 0.490:1.000.

Solvents. Five kinds of solvents, i.e., acetonitrile (Nacalai Tesque; spectrophotometric grade (S)), butyl chloride (Nacalai Tesque; guaranteed reagent (G)), ethyl acetate (Waken; G), benzene (Dojindo Laboratories; Spectrosol), and chloroform (Nacalai Tesque, S), were used as received without distillation. Table 2 shows their viscosities[27] at 20 °C and the activation energies of viscosity. The five solvents used in this study have low viscosities, 0.3–0.7 cP. We prepared the polymer solution in a quartz cell with a concentration of less than 0.1 wt %; i.e., the chromophore (anthracene) concentration was kept less than 10^{-5} M. The fluorescence lifetime and Förster radius of this chromophore are ca. 10 ns and 21.8 Å, respectively; therefore, in such a sufficiently dilute solution the energy transfer can be neglected. These samples were degassed by freeze–pump–thawing.

Table 2. Solvent Viscosity at 20 °C, Its Activation Energy, E_η, and $\bar{\alpha}_\eta^3$ for *s*- and *i*-PMMA Solutions

solvent	η/cP	E_η/ (kcal mol^{-1})	$\bar{\alpha}_\eta^3$ *s*	$\bar{\alpha}_\eta^3$ *i*
acetonitrile	0.357	1.6	0.93	0.89
butyl chloride	0.445	1.7	1.00	1.00
ethyl acetate	0.449	1.7	1.36	1.63
benzene	0.651	2.5	1.99	2.12
chloroform	0.566	1.8	2.36	2.56

Intrinsic Viscosity. We measured the intrinsic viscosity for each solution with a capillary viscometer. The polymer samples used for the measurements were *s*-PMMA (Polysciences Inc.; cat. no. 08729) and *i*-PMMA (Polysciences Inc.; cat. no. 21163). The anthracene-labeled PMMA samples prepared by GPC fractionation were not enough in quantity to afford the intrinsic viscosity measurement. We determined the molecular weight, its distribution, and the racemo fraction of these samples by GPC and ^{1}H-NMR. *s*-PMMA: M_w = 4.7 × 10^4; M_w/M_n = 1.95; racemo fraction, f_r = 0.81. *i*-PMMA: M_w = 6.5 × 10^4; M_w/M_n = 1.75; racemo fraction, f_r = 0.24. The intrinsic viscosities for both *i*-PMMA and *s*-PMMA were measured in the Θ condition, i.e., in butyl chloride at 26.5 °C for *i*-PMMA[28] and at 35.0 °C for *s*-PMMA.[29] The Θ temperature of PMMA depends on its tacticity. We evaluated the chain expansion factor, $\bar{\alpha}_\eta^3$, which is defined by $[\eta]/[\eta]_\Theta$. Table 2 also shows the value of $\bar{\alpha}_\eta^3$ at each Θ temperature.

Time-Resolved Fluorescence Depolarization Method.[30] The method is as described previously.[16] The anthryl group labeled in both *i*- and *s*-PMMA was excited by vertically polarized light of a diode laser (Hamamatsu Photonics; PLP-01) with 411 nm. The diode laser has stable power and a short pulse width of less than 50 ps. Accurate decay data of the anisotropy ratio for one sample were obtained within ca. 30 min. We collected the vertical emission intensity and the horizontal one by a single photon counting system. A microchannel plate–photomultiplier tube was used as a detector, and we could obtain a highly resolved instrumental function with fwhm = 350 ps. The time-resolved anisotropy ratio was analyzed by the same method as that reported previously.[19] The time-resolved anisotropy ratio is defined as

$$r_{obsd}(t) = (I_{VV}(t) - I_{VH}(t))/(I_{VV}(t) + 2I_{VH}(t)) \quad (1)$$

where $I_{VV}(t)$ and $I_{VH}(t)$ are the emission intensities in the vertical and horizontal direction at time t, respectively. The calculated $r_{calcd}(t)$ was made by the convolution of eq 2 with the instrumental function.

$$r(t) = r_0\{x \exp(-t/T_1) + (1 - x) \exp(-t/T_2)\} \quad (2)$$

where r_0 is the initial value of the anisotropy ratio, T_1 and T_2 are the relaxation times, and x is the fraction. Equation 2 is an empirical equation, and it shows good fitting for all the experimental data, e.g., in solvents with various viscosities or at various temperatures. The curve $r_{calcd}(t)$ was fitted to the experimental data, $r_{obsd}(t)$, by the nonlinear least-squares method. Parts a–c of Figure 3 show the fitting examples of $r_{obsd}(t)$ with $r_{calcd}(t)$. The relaxation times up to subnanosecond can be exactly evaluated by analysis with the above instruments. The mean relaxation time, T_m, is defined as

$$T_m = xT_1 + (1 - x)T_2 \quad (3)$$

The activation energy for the conformational transition, E^*, can be evaluated by using the theory of Kramers' diffusion limit.[31]

$$T_m/\eta = A \exp(E^*/RT) \quad (4)$$

The Arrhenius plot of the reduced relaxation time, T_m/η, against $1/T$ gives a straight line, and the slope corresponds to the value of E^*.

Results and Discussion

Parts a and b of Figure 4 show the Arrhenius plot of T_m/η against $1/T$ for *s*-PMMA solutions and *i*-PMMA

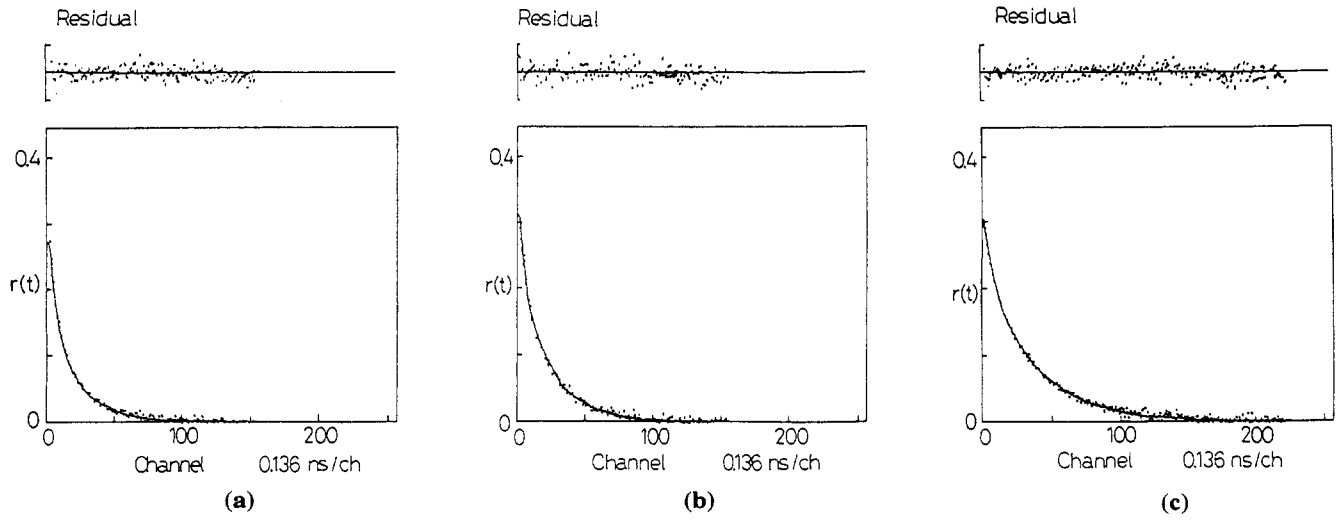

Figure 3. Decay curve of the anisotropy ratio measured for (a) *i*-PMMA in butyl chloride at 23.5 °C, (b) *s*-PMMA in butyl chloride at 34 °C, and (c) *s*-PMMA in butyl chloride at 14.7 °C. The experimental data (···) and its fitting curve by the method of nonlinear least squares (—) are given.

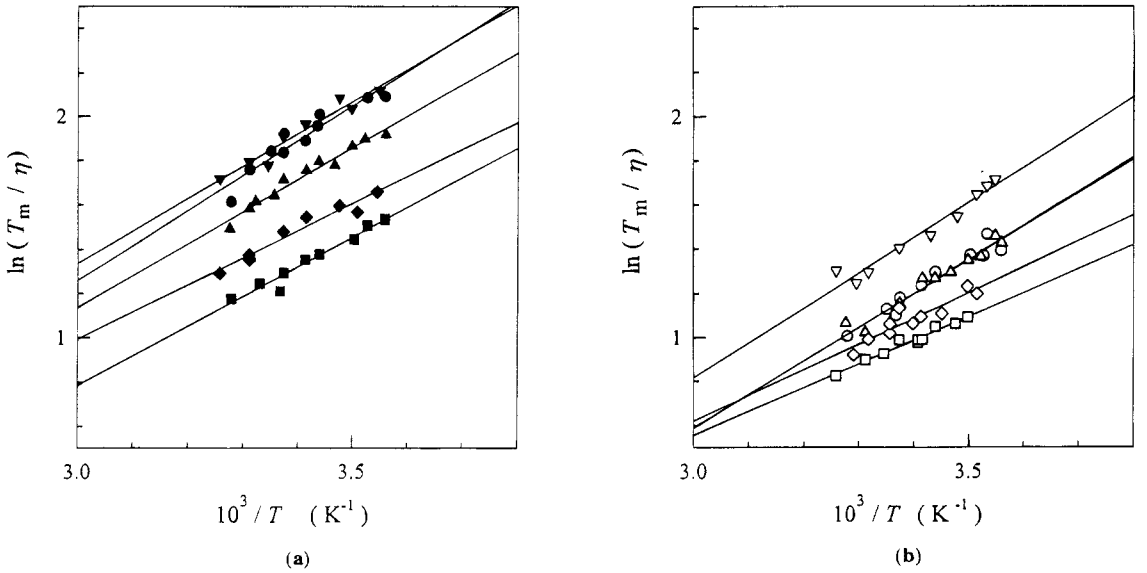

Figure 4. Plots of $\ln(T_m/\eta)$ against $1/T$: (a) for *s*-PMMA solution; (b) for *i*-PMMA solution. ○, acetonitrile; ▽, butyl chloride; △, ethyl acetate; □, benzene; ◇, chloroform.

solutions, respectively. These data clearly indicate that the relaxation time for *s*-PMMA is longer than that for *i*-PMMA.

Relationship between the Chain Dynamics and the Segment Density. First, we will consider the relationship between the relaxation time and the chain expansion factor for each polymer. Table 2 shows the value of $\bar{\alpha}_\eta^3$ as the chain expansion factor for each solution. For both polymers, the solvent quality went from poor to good in the order of acetonitrile, butyl chloride, ethyl acetate, benzene, and chloroform. Parts a and b of Figure 5 show the relationship between $\ln(T_m/\eta)$ and the local segment density at the Θ temperature for *s*-PMMA at 35 °C and *i*-PMMA at 26.5 °C, respectively. The reduced relaxation time for *s*-PMMA became shorter, with the expansion of the polymer chain. However, the T_m/η of *s*-PMMA in benzene at 35 °C was smaller than that in chloroform, though $\bar{\alpha}_\eta^3$(benzene) is smaller than $\bar{\alpha}_\eta^3$(chloroform). The cause is considered due to less solvation of benzene, not to the segment density. The same tendency was reported in another paper[32] for *s*-PMMA with a higher molecular weight (1.5×10^5). For the *i*-PMMA chain, the relaxation times similarly depended on the solvents. The value of T_m/η at 26.5 °C decreased with a decrease in the segment density. The Θ conditions of *i*-PMMA were reported to be at 26.5 °C in butyl chloride and at 27.6 °C in acetonitrile.[33] In one paper,[34] acetonitrile is also the Θ solvent at 44.0 °C for *atactic* PMMA with f_r = 0.79. We cannot explain the difference in the value of T_m/η at 26.5 °C between butyl chloride and acetonitrile, but it may be caused by a difference in the Θ conditions, e.g., solvation.

Second, we will consider the relationship between the activation energy and the chain expansion for each polymer. Parts a and b of Figure 6 show the relationship between E^* against $\bar{\alpha}_\eta^3$ for *s*-PMMA at 35 °C and for *i*-PMMA at 26.5 °C, respectively; E^* decreases with a decrease in the segment density. The value of E^* in the Θ solvent is ca. 3 kcal mol^{-1} for both *s*-PMMA and *i*-PMMA, whereas in good solvents it is 2.1–2.5 kcal mol^{-1} for both polymers. Such a difference in E^* between the Θ solvent and the good solvents was also seen for polystyrene, poly(α-methylstyrene), and poly(*p*-methylstyrene) solutions.[16]

For *s*-PMMA and *i*-PMMA, both the reduced relaxation time, T_m/η, and the activation energy, E^*, depend on the local segment density. When the segment

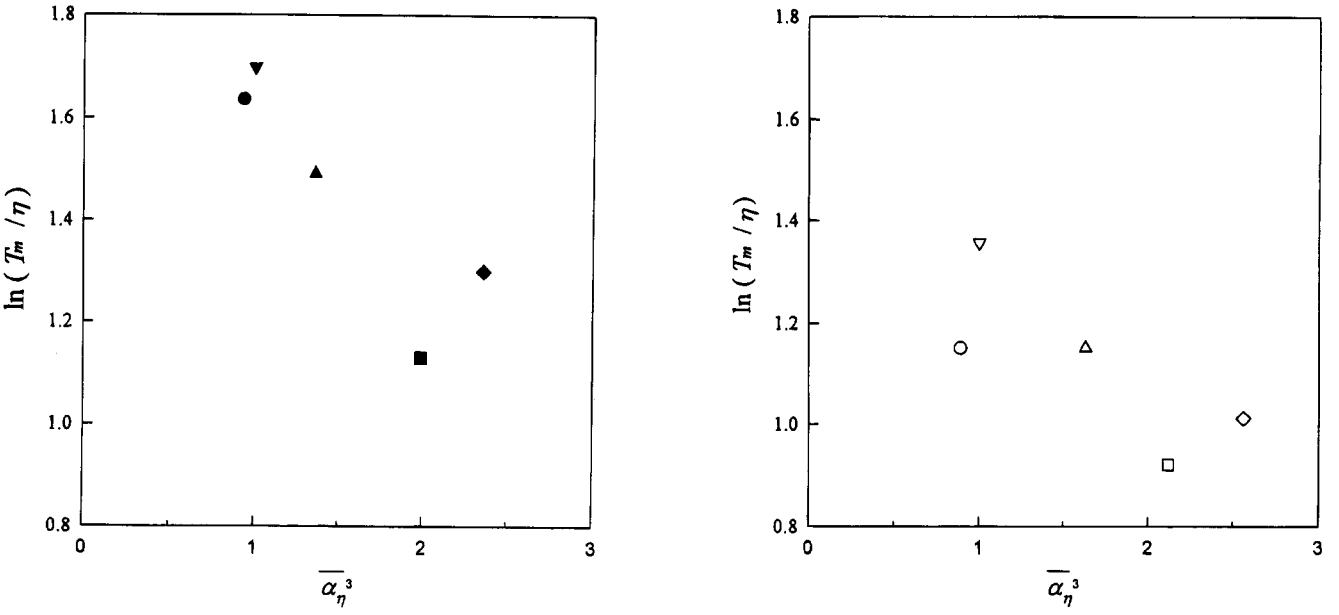

Figure 5. Plots of $\ln(T_m/\eta)$ against $\bar{\alpha}_\eta^3$: (a) for s-PMMA solution at 35.0 °C; (b) for i-PMMA solution at 26.5 °C. The symbols are the same as in Figure 4.

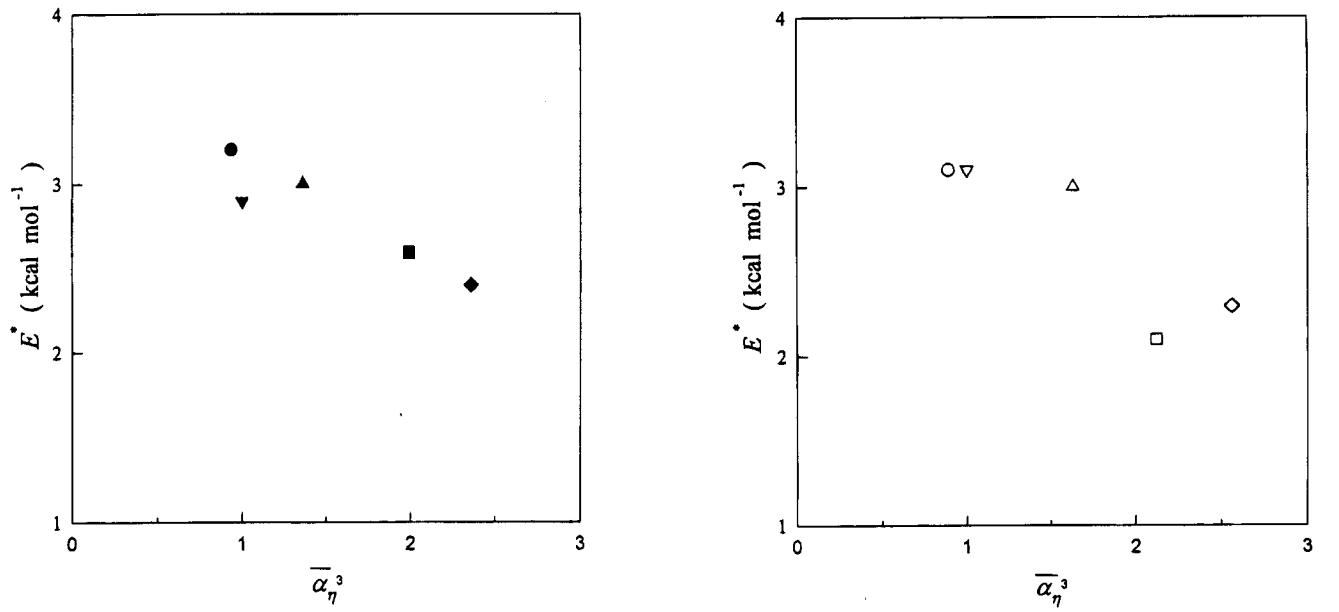

Figure 6. Plots of E^* against $\bar{\alpha}_\eta^3$: (a) for s-PMMA solution at 35.0 °C; (b) for i-PMMA solution at 26.5 °C. The symbols are the same as in Figure 4.

density is low in a good solvent, T_m/η and E^* of a PMMA chain are small, because the restriction to a chain mobility is loosened by decrement of a long-range interaction.

Dependence of the Chain Dynamics on the Tacticity. We will compare the activation energy of s-PMMA with that of i-PMMA in the same solvent. Although the segment density of s-PMMA differs from that of i-PMMA even in the same solvent, the order of the segment density in a solution among the five solvents is the same for s-PMMA and i-PMMA, and, therefore, we can compare E^* between s- and i-PMMAs in the same solvent. As Table 3 shows, E^* was almost the same for s- and i-PMMAs in the same solvent. Especially, the activation energy in the Θ solvent was independent of the kind of solvent. Although the activation energy was independent of the stereoregularity for s-PMMA and i-PMMA, it depended on the bulkiness of the substituents and the number of substitutions in the main chain, e.g., disubstitution.[16,37]

Table 3. Activation Energy, E^* (kcal mol^{-1}), for s-PMMA and i-PMMA Solutions

solvent	s-PMMA	i-PMMA
acetonitrile	3.2	3.1
butyl chloride	2.9	3.1
ethyl acetate	3.0	3.0
benzene	2.6	2.1
chloroform	2.4	2.3

Table 4 shows the difference in the relaxation time at 20 °C between i- and s-PMMA. In the Θ solvents, acetonitrile and butyl chloride, the relaxation time for s-PMMA at 20 °C was ca. 2 times larger than that for i-PMMA. In the good solvents, the relaxation time for s-PMMA at 20 °C was ca. 1.5 times larger than that for i-PMMA. The difference in the relaxation times be-

Table 4. Mean Relaxation Time, T_m (ns), at 20 °C for *s*-PMMA and *i*-PMMA Solutions

solvent	*s*-PMMA	*i*-PMMA
acetonitrile	2.4	1.2
butyl chloride	3.1	1.9
ethyl acetate	2.6	1.5
benzene	2.5	1.8
chloroform	2.5	1.7

tween *i*- and *s*-PMMA chains is closely related to the static chain stiffness which strongly depends on the chain stereoregularity.

According to the theory of HW chain by Yamakawa,[21] the static chain stiffness for a *syndiotactic* polymer chain is larger than that for an *isotactic* polymer. As the stiffness parameter, λ^{-1}, of the PMMAs by the HW chain model λ^{-1}(*s*-PMMA) = 65.6 Å and λ^{-1}(*i*-PMMA) = 32.7 Å, and the static chain stiffness of *s*-PMMA is obviously larger than that of *i*-PMMA. When the chain takes at the minimum of potential energy, the characteristic helix of the HW chain is represented by radius, ϱ, and pitch, h. Yamakawa et al. reported[35] the values of ϱ and h for *s*-PMMA and *i*-PMMA; ϱ(*s*-PMMA) = 14.4 Å, h(*s*-PMMA) = 16.5 Å, and ϱ(*i*-PMMA) = 11.4 Å, h(*i*-PMMA) = 59.3 Å. The average length of the sequences over which the tt conformation for the diads in *s*-PMMA is perpetuated is larger than that in *i*-PMMA. The actual conformation of the polymer chain in a dilute solution fluctuates by thermal motion. Then, the extent can be represented by the parameter, λ^{-1}. The larger the λ^{-1} is, the longer the regular helix is preserved. The retention of the large helical portion makes the chain stiffness of *s*-PMMA larger.[34-36]

The static chain stiffness is closely related to the local chain dynamics. Hatada et al.[24] examined the ^{13}C T_1s of *i*-PMMA (*I*:*H*:*S* = 96:4:0) and *s*-PMMA (*I*:*H*:*S* = 2:4:91) in toluene-d_8 at 110 °C by ^{13}C NMR. They also reported that the main-chain carbons in *i*-PMMA have longer T_1s than those in *s*-PMMA. This indicates the higher mobility of the main chain of *i*-PMMA compared with that of *s*-PMMA.

We found that the relaxation time depends on the chain stereoregularity but that the activation energy for the local chain motion is nearly independent of the chain stereoregularity.

Conclusion

The labeled *s*-PMMA and labeled *i*-PMMA were prepared, and the relaxation times for these polymers in various solvents were measured by the fluorescence depolarization method. As for both polymers, the segment density of a polymer chain depends on the solvent quality, which determines a long-range interaction between polymer chains and gives the large effect on the local chain motion, i.e., the higher the segment density is, the larger the values of T_m and E^* are. This indicates that the polymer chain in a poor solvent is compacted and its local motion depends strongly on the long-range interaction. In good solvents the values of T_m and E^* for PMMA chain are smaller, because a long-range interaction in a chain is weaker and the restriction to a conformational transition is loosened.

Comparison of the T_m of *i*-PMMA with that of *s*-PMMA at 20 °C revealed that the T_m of *s*-PMMA is 1.5–2.0 times longer than that of *i*-PMMA. The stereoregularity is one of the important factors governing local chain dynamics as well as chain conformation and static chain stiffness. Chain conformation of *s*-PMMA with the retention of a large helical portion makes the chain stiffness larger than that for *i*-PMMA, and probably the static chain stiffness is closely related to the relaxation time of the local motion. However, E^* for *s*-PMMA was similar to that for *i*-PMMA, and the activation energy was almost independent of the stereoregularity. More detailed studies of this mechanism are being carried out.

Acknowledgment. The present work was supported by a Grant-in-Aid for Scientific Research on Priority Areas, Photochemical Reactions (No. 06239107) from the Ministry of Education, Science and Culture of Japan.

References and Notes

(1) (a) Rouse, P. E., Jr. *J. Chem. Phys.* **1953**, *21*, 1272. (b) Zimm, B. H. *J. Chem. Phys.* **1956**, *24*, 269.
(2) Ferry, J. D. *Viscoelastic Properties of Polymers*, 3rd ed.; John Wiley & Sons, Inc.: New York, 1980; Chapter 9.
(3) Helfand, E. *J. Chem. Phys.* **1971**, *54*, 4651.
(4) Heatley, F. *Prog. NMR Spectrosc.* **1979**, *13*, 47.
(5) Lauprêtre, F.; Noël, C.; Monnerie, L. *J. Polym. Sci., Polym. Phys. Ed.* **1977**, *15*, 2127.
(6) Bullock, A. T.; Cameron, G. G.; Smith, P. M. *J. Chem. Soc., Faraday Trans. 2* **1974**, *70*, 1202.
(7) Shiotani, M.; Sohma, J.; Freed, J. H. *Macromolecules* **1983**, *16*, 1495.
(8) Mashimo, S.; Winsor, P., IV; Cole, R. H.; Matsuo, K.; Stockmayer, W. H. *Macromolecules* **1986**, *19*, 682.
(9) Adachi, K. *Macromolecules* **1990**, *23*, 1816.
(10) Higgins, J. S.; Maconnachie, A. In *Methods of Experimental Physics*; Sköld, K., Price, D. L., Eds.; Academic Press: New York, 1987; Vol. 23, Part C, p 287.
(11) Chu, B. *Laser Light Scattering*, 2nd ed.; Academic Press: New York, 1991.
(12) Valeur, B.; Monnerie, L. *J. Polym. Sci., Polym. Phys. Ed.* **1976**, *14*, 11.
(13) Ediger, M. D. *Annu. Rev. Phys. Chem.* **1991**, *42*, 225.
(14) Sasaki, T.; Yamamoto, M. *Macromolecules* **1989**, *22*, 4009.
(15) Ono, K.; Okada, Y.; Yokotsuka, S.; Ito, S.; Yamamoto, M. *Polym. J.* **1994**, *26*, 199.
(16) Ono, K.; Okada, Y.; Yokotsuka, S.; Sasaki, T.; Yamamoto, M. *Macromolecules* **1994**, *27*, 6482.
(17) Sasaki, T.; Yamamoto, M.; Nishijima, Y. *Macromolecules* **1988**, *21*, 610.
(18) Sasaki, T.; Arisawa, H.; Yamamoto, M. *Polym. J.* **1991**, *23*, 103.
(19) Ono, K.; Ueda, K.; Yamamoto, M. *Polym. J.* **1994**, *26*, 1345.
(20) Yamakawa, H. *Macromolecules* **1977**, *10*, 692.
(21) Fujii, M.; Nagasaka, K.; Shimada, J.; Yamakawa, H. *Macromolecules* **1983**, *16*, 1613.
(22) Yoshizaki, T.; Yamakawa, H. *J. Chem. Phys.* **1984**, *81*, 982.
(23) Iwasa, Y.; Mashimo, S.; Chiba, A. *Polym. J.* **1976**, *8*, 401.
(24) Hatada, K.; Kitayama, T.; Terawaki, Y.; Ohta, K.; Okamoto, Y.; Yuki, H.; Lenz, R. W. *Bull. Inst. Chem. Res., Kyoto Univ.* **1988**, *66*, 115.
(25) (a) Yuki, H.; Hatada, K.; Niinomi, T.; Kikuchi, Y. *Polym. J.* **1970**, *1*, 36. (b) Okamoto, Y.; Ohta, K.; Hatada, K.; Yuki, H. *ACS Symp. Ser.* **1981**, *166*, 353. (c) Doherty, M. A.; Hogen-Esch, T. E. *Makromol. Chem.* **1986**, *187*, 61.
(26) Later, it has been found that a prolonged stirring (for 84 h) at −20 °C gives a more satisfactory result on the coupling reaction of the living poly(TrMA) anions with 9,10-bis(bromomethyl)anthracene.
(27) *Kagaku Binran Kiso Hen*, 3rd ed.; The Chemical Society of Japan, Ed.; Maruzen: Tokyo, 1984; Vol. II, Chapter 6.
(28) Schulz, G. V.; Wunderlich, W.; Kirste, R. G. *Makromol. Chem.* **1964**, *75*, 22.
(29) Kirste, R. G.; Schulz, G. V. *Z. Phys. Chem.* **1961**, *27*, 310.
(30) (a) Weber, G. *Biochemistry* **1952**, *51*, 145. (b) O'Conner, D. V.; Phillips, D. *Time-Correlated Single-Photon Counting*; Academic Press: London, 1984.
(31) Kramers, H. A. *Physica* **1940**, *7*, 284.
(32) Horinaka, J.; Ono, K.; Yamamoto, M. *Polym. J.* **1995**, *27*, 429.
(33) Krause, S.; Cohn-Ginsberg, E. *J. Phys. Chem.* **1963**, *67*, 1479.
(34) Tamai, Y.; Konishi, T.; Einaga, Y.; Fujii, M.; Yamakawa, H. *Macromolecules* **1990**, *23*, 4067.
(35) Yamakawa, H.; Shimada, J. *J. Chem. Phys.* **1979**, *70*, 609.
(36) Yoon, D. Y.; Flory, P. J. *J. Polym. Sci., Polym. Phys. Ed.* **1976**, *14*, 1425.
(37) Ono, K.; Ueda, K.; Sasaki, T.; Murase, S.; Yamamoto, M. *Macromolecules* Submitted.

MA946281A